100-340GHz Spatially Multiplexed Communications: IC, Transceiver, and Link Design

Mark J.W. Rodwell
University of California, Santa Barbara, USA, email: rodwell@ece.ucsb.edu

***Abstract*—**We describe the opportunities, and the research challenges, presented in the development of 100-340GHz wireless communications and imaging systems. In such links, short wavelengths permit massive spatial multiplexing both for network nodes and point-point links. 100-340GHz imaging systems can provide tens of thousands of image pixels and ~0.1° angular resolution from small apertures, supporting foul-weather driving and aviation.

I. Introduction

Wireless networks face exploding demand; the available spectrum is nearly exhausted. Industry is responding by introducing 5G systems at 28, 38, 57-71(WiGig), and 71-86GHz. Research now considers next-generation systems between 100-340 GHz. These will access a much larger spectrum. The short wavelengths provide massive spatial multiplexing in hub and backhaul communications. The short wavelengths will permit high-resolution imaging, from small apertures, to assist driving or flying in foul weather.

One potential application is high-capacity mobile communication (Figure 1a), with spatially multiplexed mm-wave base stations (network hubs) providing endpoint (user) connections, and with network backhaul on a mix of optical fiber and high-capacity spatially multiplexed mm-wave links. Similar networks might provide high-capacity network connections to residences and offices

A second potential application is transportation (Figure 1b), supporting self-driving cars and intelligent highways. mm-wave imaging radar, at e.g. 220 or 340GHz, can provide TV-like resolution to see through fog and rain. Coupled with a heads-up display, such a system might aid driving, whether by human or autonomous system, in foul-weather conditions where visibility is very poor.

A third application is in sensing and imaging for aviation and for national security, identifying threats through fog/smoke/dust, when one cannot see in the optical. Microwave radar provides longer range but lower resolution, detecting threats at long-range. 140-340GHz imaging radar would serve for threat identification, providing shorter range (~500m in fog), but TV-like resolution, even from a small aperture which can fit on a jeep, helicopter, or UAV.

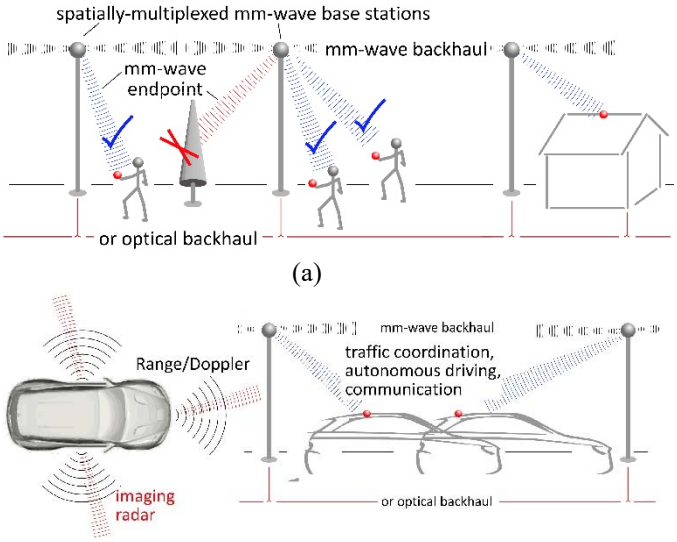

Figure 1: mm-wave/THz applications: (a) spatially multiplexed networks for multi-Gigabit mobile and residential/office communication and (b) THz radar and imaging systems supporting autonomous cars and driving in foul weather, with wideband links between cars and highway infrastructure to coordinate traffic.

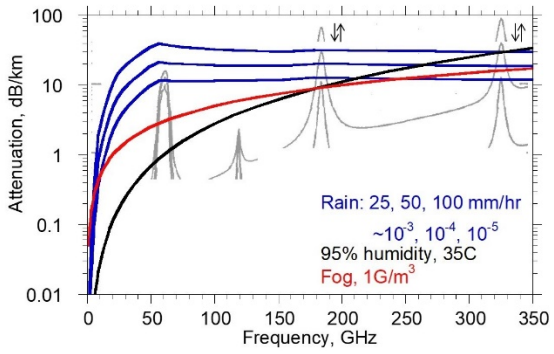

Figure 2: Approximate sketch of atmospheric attenuation vs. frequency and weather, drawn from references [1-4]. Attenuation in the vicinity of the 120, 180, and 325GHz absorption lines is not accurately represented.

II. 100-340 GHz Systems

100-340GHz systems can provide very high data capacity. In clear weather, there are large bandwidths at 125-165GHz and 200-300 GHz between absorption lines, and a narrower window near 340GHz. Phased array transceivers, whether in network hubs (Figure 3) or in point-point links (Figures 4,5) can provide, in a given bandwidth, multiple simultaneous independent beams,

carrying independent modulation, with an angular resolution proportional to $\lambda/$(array width) . This spatial multiplexing implies massive spectral re-use, and the potential for very high communications capacity. Critically, short wavelengths permit this in arrays of reasonable size. Similarly, in imaging radar (Figure 6), short wavelengths permit fine angular resolution, and very many image pixels, from arrays small enough to fit on a car or small aircraft.

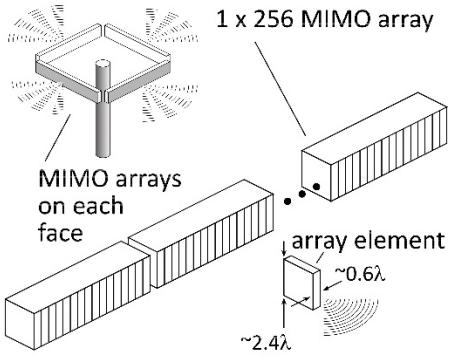

Figure 3: Spatially multiplexed network hub. The hub has 4 faces, each a 256-element MIMO array, providing up to 128 independent signal beams. Link SNR analysis suggests that, with a 140GHz carrier at 100m range, 10Gb/s transmission per beam is feasible

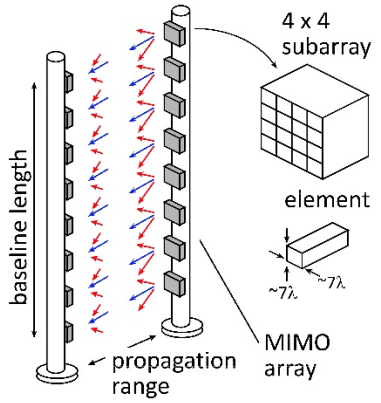

Figure 4: Spatially multiplexed wireless backhaul link, using linear transmitter and receiver array, with each element being a 4×4 subarray

Unfortunately, propagation loss is high, both from λ^2/R^2 propagation losses and from foul-weather attenuation. Between 50-1000GHz, rain attenuation [1,2] is <30-35 dB/km with 99.999% probability and <18-26 dB/km with 99.99% probability. At least below ~500GHz rain attenuation dominates over that of fog [3], though attenuation due to humidity [4] dominates above ~250GHz. References [1-4] summarize well the Consequently, 100-340 GHz outdoor terrestrial links must tolerate perhaps 20 dB/km attenuation: link range is necessarily short. Further, the area $\sim \lambda R$ of the first Fresnel zone is small, hence beams are easily blocked. Phased array transceivers are necessary both for adequate transmission range (given the necessary small beam width, fix-aimed high-gain antennas are expensive to install) and to provide *adaptive beam steering* in *mesh networks* to accommodate beam blockage.

Consider three example applications: a wireless communications hub serving 100's of mobile users [5,6,7] , a spatially multiplexed point-point backhaul link, connecting such hubs to the network backbone, and an imaging system, with TV-like resolution, enabling driving in very heavy fog or rain.

Figure 3 shows a 140GHz spatially multiplexed hub, supporting 512 users. Each of 4 hub faces has 256 antennas, each 0.6λ × 2.4 λ, in a 0.35m length phased array. We analyze the system using the Friis equation [8] $P_{received}/P_{trans} = (D_t D_r/16\pi^2)(\lambda/R)^2 \exp(-\alpha R)$, where the antenna directivities are $D = 4\pi A_{eff}/\lambda^2$ and A_{eff} are the antenna array aperture areas. We assume uncoded QPSK modulation at 10^{-3} error rate, which implies $P_{received} = Q^2 kTFB$, where B is the bit rate and Q^2 =SNR=9.5 (9.8dB). The required output power per element is then $P_{element} = P_{transmit}(m/n)$, where m is the number of signal beams and n the # of transmit array elements. Assume a handset with an 8×8 array, at λ/2 spacing (9mm×9mm), 20 dB margins for packaging, manufacturing, aging, and partial beam obstruction. A 45 mW transmitter output power per element and 3 dB handset noise figure can then support 128 users per array face, at up to 100m range, and 10Gb/s downlink rate per user, even in 50mm/hr. rain. The 140GHz link has similar range to a 75GHz link having the same transmit power and receive noise figure, a hub array of the same directivity, and a handset array of the same physical area.

Figure 4 shows a spatially multiplexed backhaul link. N transmitters, carrying independent data, form an array of length L. The receiver, at distance R, has a similar array but uses line-of-sight MIMO [9] beamforming. If the array angular resolution λ/L is smaller than the element apparent angular separation L/NR, then the signals can recovered with high SNR. Link capacity is increased N:1. Short wavelengths are of great advantage, as a short array can then carry many channels; at 500m range, an 8-element array must be 1.6m long at 340GHz, 2.6m at 140GHz, and 3.5m at 75GHz. At 340GHz, if each array element is an 8×8 subarray of 7λ by 7λ elements (for small beam angle adjustment) then, with 20 dB total margins and QPSK at 10^{-3} error rate, transmitting 640Gb/s over 500m range in 50mm/hr. rain requires only 80 mW/element output power, and 4dB receiver noise figure. Using two polarizations, the capacity is 1.2Tb/s in the same length array. At 140GHz, only 2mW/element is required, but the superarray must be longer.

Figure 5 shows a point-point link using rectangular line-of-sight MIMO arrays. At 340GHz and over 500m range, providing 5Tb/s capacity given 80Gb/s per subarray, would require a 1.6m × 1.6 meter, 64-element

superarray. With assumptions as in the prior example, each sub-element need radiate only 10mW. Note, however, that the lower-capacity linear array fits more easily on a utility pole or light pole.

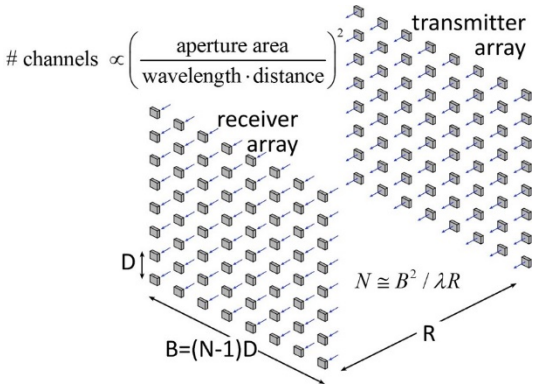

Figure 5: Spatial multiplexing in a line-of-sight mm-wave MIMO link, in this case with a square array. Here the capacity varies as the product of the channel bandwidth and the square of the carrier frequency.

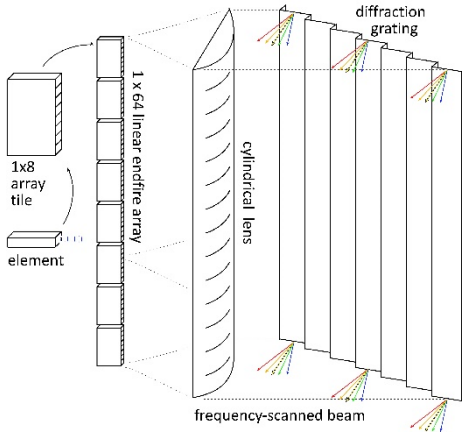

Figure 6: 340 GHz frequency-scanned imaging radar for driving in foul weather. The figure shows a separate imaging lens and diffraction grating for lateral beamsteering; these can be combined into a Fresnel lens.

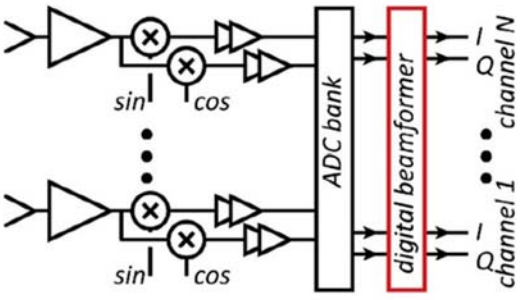

Figure 7: Sketch of the RF through baseband signal chain, with digital beamforming, for the massive MIMO receiver of figure 2. The transmitter is similar, with digital beamformer, DAC bank, (I,Q) baseband to RF upconversion, power amplifiers, and antennas.

The third example (Figure 6) is 340GHz imaging radar, for driving in e.g. heavy fog, providing a TV-like 64×512 pixel image refreshed at 60Hz. A linear 1×64 array steers the beam vertically, while frequency scanning and a frequency-selective Fresnel lens steers it horizontally. From the radar range equation, given a 35cm×35cm aperture, 10dB systems margin, 10% pulse duty factor, and 10dB SNR from a 1 ft^2 , 10% reflectivity target at 300m range in heavy fog, the necessary peak output power is 50mW/element given 7.5dB receiver noise. The high 340GHz carrier permits a sharp 0.14 degree resolution from an array that can fit behind a car's radiator grille.

III. IC Technologies for the RF Front End

The IC technologies needed to realize these system are available today; further improvements will improve receiver sensitivity and transmitter output power and efficiency. The required RF components (Figure 7) include low-noise amplifiers (LNAs), IQ downconversion mixers, and LO sources (multipliers or PLLs) and LO drive amplifiers in the receivers, plus efficient power amplifiers (PAs) in the transmitters. In CMOS VLSI, high-performance RF-front-ends can be realized at 140GHz [10], and possibly at 240GHz [11], though realizing quality amplifiers at 240GHz is extremely challenging. Even at 140GHz, CMOS PA output power will be very limited, c.a. 10dBm. SiGe BiCMOS offers higher PA output power and higher operating frequencies [12, 13], but the higher-frequency results are in R&D technologies. Present commercially-available foundry SiGe technologies are useful to only c.a. 200GHz. InP HBT technologies, in low-volume pilot production for aerospace applications, have realized ICs to 650GHz [14]. Useful IC performance is at somewhat lower frequencies, with ~200 mW PAs (Figure 8) at 215GHz [15, 16] and 22mW PAs at 340GHz [17]. 1.0 THz monolithic amplifiers have been demonstrated using InP HEMTs [18], and such devices can offer 2-4 dB (device-level) noise figures at 140-340GHz. The more advanced R&D GaN HEMT technologies [19] produce extremely large power densities at 94GHz; it is expected that, with moderate improvement, these will permit high-power PAs at 140GHz and perhaps 220GHz.

With IC technologies available today from high-volume commercial foundries, 140GHz and perhaps 220GHz transceivers with output power sufficient for outdoor applications can be realized in SiGe, or in CMOS with SiGe PAs. As R&D InP, GaN and advanced (faster) SiGe technologies mature and enter high-volume production, 220GHz and 340GHz systems will be more easily realized.

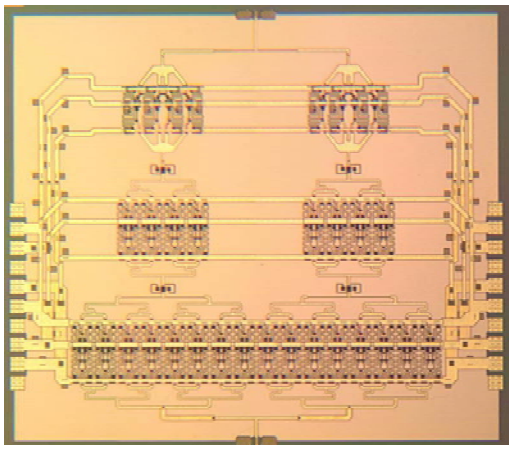

Figure 8: 180mW, 220 GHz InP Power Amplifier [15].

IV. Array Tile, Antenna, and Package Design

100-340GHz array transceivers present formidable challenges in packaging. To steer over 180° both in azimuth and elevation, the array must be 2-dimensional and must have $\sim \lambda / 2$ element spacing, 1mm at 140GHz and 0.4mm at 340GHz. It is difficult to fit the necessary per-channel RF electronics in a small 1mm×1mm area, particularly if high-power PAs are required, and it is difficult to remove the heat. High-frequency IC connections are also difficult.

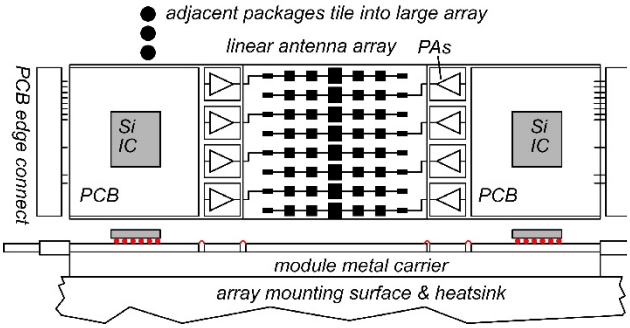

Figure 9: Array tile design for linear arrays providing beam steering in azimuth but not elevation (the image has been rotated 90° to make it fit in the document) in the MIMO hub of figure 2.

If the users (Figure 1) are distributed over the ground, then the array need steer only in azimuth, and can be 1-dimensional (Figure 3). The RF beamforming electronics, LNAs, and PAs, can then be placed along the outside edges of the antenna array, providing sufficient space for moderately large ICs even at 340GHz. As in standard in radar, the large MIMO array is formed from smaller array tile modules. In a 1-D array, the ICs and antennas can be mounted on metal trays within the array tile, and the tiles mounted on a large metal backplane and heatsink. In this way, heat from even high-power amplifiers can be removed with an adequately low temperature rise.

In backhaul links (Figure 4), the communicating transceivers are fixed rigidly to the ground. Phased-array electronic beamsteering, using the subarray, is nevertheless desired, as this allows automatic beam aiming, avoiding high labor cost of precision aiming of a high-directivity antenna. Because the necessary angular beamsteering range is only c.a. 10°, subarray elements can be widely spaced, by ~7λ. Figure 10a shows an array tile design for this application, with linear arrays of Vivaldi endfire antennas, plus PAs/LANs and beamforming ICs mounted on a metal tray to form the array tile. A two-dimensional array of tiles can then be mounted on a metal backplane/heatsink to form the overall MIMO or imaging array. At 7λ spacing, the array tile pitch is sufficient for the metal tray to be several mm thick even in a 340GHz design; this allows heat to be carried from the PAs and beamformer ICs to the backplane heatsink with low thermal resistance. Alternately, such tiles can be placed in a linear array for frequency-scanned imaging (Figure 6).

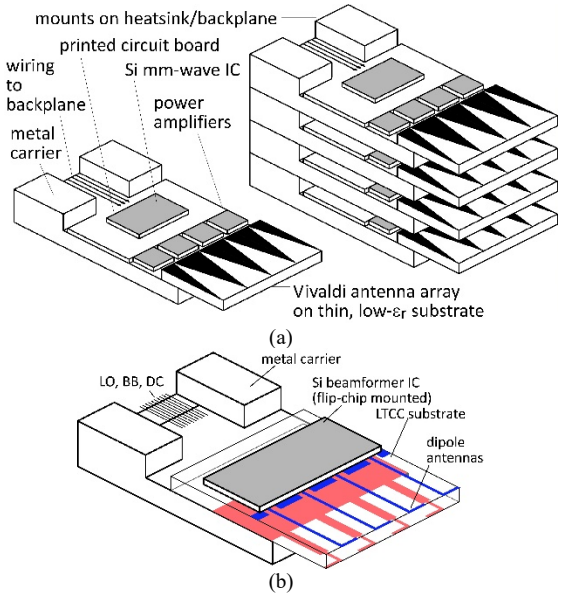

Figure 10: Array tile designs for 2D array, consisting of a metal tray/heatsink, a Si beamformer IC mounted on an e.g. LTCC carrier, and an endfire antenna array on a low-ε_r substrate. (a) Array tile design with ~7λ spacing for small-angular-deviation 2D beamsteering in fix-aimed point-point links, (b) and design with ~λ/2 spacing for wide-angular-deviation 2D beamsteering in imaging and mobile applications.

The most challenging package design is for arrays which must aim over wide angles both in azimuth and elevation. In this case the element spacings must be ~λ/2. One possible array tile design (Figure 10B) would use ~λ/2 dipole antennas (with a backshort reflector) on a dielectric substrate. The package design is similar to the narrow-steering-range tile design (Figure 10A), but the element spacings are much smaller. In particular, above 140GHz the metal tray must be made very thin to permit λ/2 spacing, and PA heatsinking is then compromised. Array tile designs using split-block waveguide techniques

may be necessary to address 2D, widely-steerable arrays in systems operating above 140GHz.

V. Systems Architectures and Challenges

Common to most of these systems is massive spatial multiplexing. In the transmitter, the signals driving the many (of order 100) antennas must be formed as separate linear combinations of the many (of order 100) signals to be transmitted. The receiver must perform a similar matrix operation, with many signal channels and high symbol rates.

In an all-digital [20] beamforming architecture (Figure 7), whether transmitter or receiver, nonlinearities in the analog (RF-baseband) signal chain, ADC/DAC quantization errors, and local oscillator phase noise all introduce user-user or channel-channel crosstalk, potentially reducing the system capacity. Yet, with moderate power control and QPSK modulation, we find that the ADC/DAC resolution can be quite coarse [21], and that the analog chain 1dB gain compression point need not be markedly greater than the average signal power levels. Similarly, we find [22], that the maximum tolerable LO phase noise in massive MIMO links does not differ significantly from that tolerable in SISO links of comparable symbol rates and constellations. The minimum necessary computational complexity of the digital beamformer is an area of active investigation.

Acknowledgment

This work was supported in part by the Semiconductor Research Corporation and DARPA under the JUMP program

References

[1] R. Olsen, D. Rogers, D. Hodge, IEEE Trans. Antennas and Propagation, , vol.26, no.2, pp. 318- 329, Mar 1978

[2] Y. Karasawa, Y.Maekawa, "Ka-band Earth-space propagation research in Japan" Proceedings of the IEEE , Volume: 85 , Issue: 6 , June 1997 Pages:821 - 84

[3] H.J Liebe, T. Manabe, G.A. Hufford, IEEE Transactions on Antennas and Propagation, Volume: 37 , Issue: 12 , Dec. 1989

[4] M. J. Rosker, H. B. Wallace, "Imaging Through the Atmosphere at Terahertz Frequencies," 2007 IEEE MTT-S International Microwave Symposium, 3-8 June.

[5] Marzetta, T. L., Larsson, E. G., Edfors, O., & Tufvesson, F. (2014). Massive MIMO for Next Generation Wireless Systems. IEEE Communications Magazine, 52(2), 186-195.

[6] A. L. Swindlehurst, *et al*. "Millimeter-wave massive MIMO: The next wireless revolution?." IEEE Communications Magazine 52.9 (2014): 56-62.

[7] Hoydis, Jakob, Stephan Ten Brink, and Mérouane Debbah. "Massive MIMO in the UL/DL of cellular networks: How many antennas do we need?." IEEE Journal on selected Areas in Communications 31, no. 2 (2013): 160-171.

[8] H. T. Friis, "A note on a simple transmission formula," Proc. IRE 34, 254–256 (1946).

[9] C. Sheldon, M. Seo, E. Torkildson, M. Rodwell and U. Madhow, "Four-channel spatial multiplexing over a millimeter-wave line-of-sight link," 2009 IEEE International Microwave Symposium, Boston, MA,.

[10] A. Simsek, S. Kim and M. J. W. Rodwell, "A 140 GHz MIMO Transceiver in 45 nm SOI CMOS," 2018 IEEE BiCMOS and Compound Semiconductor Integrated Circuits and Technology Symposium (BCICTS), San Diego, CA, 2018, pp. 231-234.

[11] S. Thyagarajan, S. Kang, and A. Niknejad, "A 240 GHz wideband QPSK receiver in 65 nm CMOS," in Proc. Radio Freq. Integr. Circuits Symp., 2014, pp. 357–360.

[12] B. Heinemann et al., "SiGe HBT with ft/fmax of 505 GHz/720 GHz," 2016 IEDM, San Francisco, CA, 2016, pp. 3.1.1-3.1.4.

[13] J. Al-Eryani, H. Knapp, J. Kammerer, K. Aufinger, H. Li and L. Maurer, "Fully Integrated Single-Chip 305–375-GHz Transceiver With On-Chip Antennas in SiGe BiCMOS," in IEEE Transactions on Terahertz Science and Technology, vol. 8, no. 3, pp. 329-339, May 2018.

[14] M. Urteaga, Z. Griffith, M. Seo, J. Hacker and M. J. W. Rodwell, "InP HBT Technologies for THz Integrated Circuits," IEEE Proceedings, vol. 105, no. 6, pp. 1051-1067, June 2017

[15] T. B. Reed, Z. Griffith, P. Rowell, M. Field and M. Rodwell, "A 180mW InP HBT Power Amplifier MMIC at 214 GHz," 2013 IEEE Compound Semiconductor Integrated Circuit Symposium (CSICS), Monterey, CA

[16] Z. Griffith, M. Urteaga and P. Rowell, "180–265 GHz, 17–24 dBm output power broadband, high-gain power amplifiers in InP HBT," 2017 IEEE MTT-S International Microwave Symposium (IMS), Honolulu, HI, 2017, pp. 973-976.

[17] J. Kim, S. Jeon, M. Kim, M. Urteaga and J. Jeong, "H-Band power amplifier integrated circuits using 250-nm InP HBT technology," in IEEE Transactions on Terahertz Science and Technology, vol. 5, no. 2, pp. 215-222, March 2015

[18] W. R. Deal, K. Leong, W. Yoshida, A. Zamora and X. B. Mei, "InP HEMT integrated circuits operating above 1,000 GHz," 2016 IEEE International Electron Devices Meeting (IEDM), San Francisco, CA, 2016, pp. 29.1.1-29.1.4.

[19] S. Wienecke et al., "N-Polar GaN Cap MISHEMT With Record Power Density Exceeding 6.5 W/mm at 94 GHz," IEEE Electron Device Letters, vol. 38, no. 3, pp. 359-362, March 2017.

[20] T.E. Bogale, L.B.Le, "Beamforming for multiuser massive MIMO systems: Digital versus hybrid analog-digital", 2014 IEEE Global Communications Conference

[21] M. Abdelghany, A. A. Farid, U. Madhow and M. J. W. Rodwell, "Towards All-digital mmWave Massive MIMO: Designing around Nonlinearities," 2018 52nd Asilomar Conference on Signals, Systems, and Computers, Pacific Grove, CA, USA, 2018, pp. 1552-1557.

[22] M. E. Rasekh *et al.*, " Phase Noise Analysis for mmwave Massive MIMO: a Design Framework for Scaling via Tiled Architectures", *to be presented*, 53rd Annual Conference on Information Systems & Sciences, Johns Hopkins University, Baltimore, Maryland, March 20-22, 2019